Time-of-Flight Secondary Ion Mass Spectrometry Imaging of Subcellular Lipid Heterogeneity: Poisson Counting and Spatial Resolution

ARTICLE *in* ANALYTICAL CHEMISTRY · JULY 2009

Impact Factor: 5.64 · DOI: 10.1021/ac901065s · Source: PubMed

7 AUTHORS, INCLUDING:

Paul Piehowski
Pacific Northwest National Laboratory
21 PUBLICATIONS **302** CITATIONS
SEE PROFILE

Michael E. Kurczy
AstraZeneca
34 PUBLICATIONS **474** CITATIONS
SEE PROFILE

Erin D Sheets
University of Minnesota Duluth
32 PUBLICATIONS **2,273** CITATIONS
SEE PROFILE

Andrew G Ewing
University of Gothenburg
191 PUBLICATIONS **5,348** CITATIONS
SEE PROFILE

Anal. Chem. **2009,** *81,* 5593–5602

Time-of-Flight Secondary Ion Mass Spectrometry Imaging of Subcellular Lipid Heterogeneity: Poisson Counting and Spatial Resolution

Paul D. Piehowski,[†] Angel M. Davey,[†] Michael E. Kurczy,[†] Erin D. Sheets,[†] Nicholas Winograd,[†] Andrew G. Ewing,[†,‡] and Michael L. Heien*[,†]

Department of Chemistry, The Pennsylvania State University, University Park, Pennsylvania 16802, and Department of Chemistry, Göteborg University, Kemivägen 10, SE-41296 Göteborg, Sweden

Mass spectrometric imaging is a powerful tool to interrogate biological complexity. One such technique, time-of-flight secondary ion mass spectrometry (TOF-SIMS) imaging, has been successfully utilized for subcellular imaging of cell membrane components. In order for this technique to provide insight into biological processes, it is critical to characterize the figures of merit. Because a SIMS instrument counts individual events, the precision of the measurement is controlled by counting statistics. As the analysis area decreases, the number of molecules available for analysis diminishes. This becomes critical when imaging subcellular features; it limits the information obtainable, resulting in images with only a few counts of interest per pixel. Many features observed in low intensity images are artifacts of counting statistics, making validation of these features crucial to arriving at accurate conclusions. With TOF-SIMS imaging, the experimentally attainable spatial resolution is a function of the molecule of interest, sample matrix, concentration, primary ion, instrument transmission, and spot size of the primary ion beam. A model, based on Poisson statistics, has been developed to validate SIMS imaging data when signal is limited. This model can be used to estimate the effective spatial resolution and limits of detection prior to analysis, making it a powerful tool for tailoring future investigations. In addition, the model allows comparison of pixel-to-pixel intensity and can be used to validate the significance of observed image features. The implications and capabilities of the model are demonstrated by imaging the cell membrane of resting RBL-2H3 mast cells.

Imaging with time-of-flight secondary ion mass spectrometry (TOF-SIMS) is a powerful analytical tool for mapping the spatial distribution of biologically relevant small molecules (<1000 Da) on a surface.[1] Because of the inherent surface sensitivity of the technique, TOF-SIMS has been used for the study of cell membrane lipids, such as phospholipids and cholesterol.[2−5] Primary ion sources employed for TOF-SIMS experiments are not diffraction-limited and thus provide nanometer-scale spatial resolution.[6−9] The desorbed ions are analyzed using TOF, which provides high chemical specificity. Recent advances in MS instrumentation used to analyze secondary ions promise to greatly increase the chemical specificity available for imaging experiments.[10,11] When combined with cryogenic sample preparation techniques, TOF-SIMS permits the detailed study of membrane lipids during dynamic processes such as membrane fusion.[12−14]

The capability of TOF-SIMS to image subcellular features of the plasma membrane has been previously demonstrated; however, these features were significantly larger than the minimum pixel size available for the analysis.[2,3] Further, these features appeared in distinct cellular locations on the cell that allowed for features to be easily identified via a line scan (a plot of the signal intensity for a given ion as a function of its lateral position on the line). Analyzing small features becomes difficult as feature size approaches the minimum pixel size, an experimental limit imposed by the focus of the primary ion beam. Indeed, when characterizing these small features, signal averaging cannot be used, making it necessary to compare fewer pixels to one another. The concept of useful lateral resolution, ΔL, has long existed in the SIMS community.[15] ΔL is defined as the side of the minimum square area in which N secondary ions of a given mass can be desorbed

* Corresponding author. Michael L. Heien, e-mail: mheien@psu.edu.
[†] The Pennsylvania State University.
[‡] Göteborg University.

(1) Johansson, B. *Surf. Interface Anal.* **2006**, *38*, 1401–1412.
(2) Ostrowski, S. G.; Bell, C. T. V.; Winograd, N.; Ewing, A. G. *Science* **2004**, *305*, 71–73.
(3) Monroe, E. B.; Jurchen, J. C.; Lee, J.; Rubakhin, S. S.; Sweedler, J. V. *J. Am. Chem. Soc.* **2005**, *127*, 12152–12153.
(4) Nygren, H.; Malmberg, P. *Trends Biotechnol.* **2007**, *25*, 499–504.
(5) Altelaar, A. F. M.; van Minnen, J.; Jimenez, C. R.; Heeren, R. M. A.; Piersma, S. R. *Anal. Chem.* **2005**, *77*, 735–741.
(6) Marxer, C. G.; Kraft, M. L.; Weber, P. K.; Hutcheon, I. D.; Boxer, S. G. *Biophys. J.* **2005**, *88*, 2965–2975.
(7) Kraft, M. L.; Weber, P. K.; Longo, M. L.; Hutcheon, I. D.; Boxer, S. G. *Science* **2006**, *313*, 1948–1951.
(8) Winograd, N. *Anal. Chem.* **2005**, 143A–149A.
(9) Peteranderl, R.; Lechene, C. *J. Am. Soc. Mass Spectrom.* **2004**, *15*, 478–485.
(10) Carado, A.; Passarelli, M. K.; Kozole, J.; Wingate, J. E.; Winograd, N.; Loboda, A. V. *Anal. Chem.* **2008**, *80*, 7921–7929.
(11) Fletcher, J. S.; Rabbani, S.; Henderson, A.; Blenkinsopp, P.; Thompson, S. P.; Lockyer, N. P.; Vickerman, J. C. *Anal. Chem.* **2008**, *80*, 9058–9064.
(12) Roddy, T. P.; Donald, M.; Cannon, J.; Meserole, C. A.; Winograd, N.; Ewing, A. G. *Anal. Chem.* **2002**, *74*, 4011–4019.
(13) Roddy, T. P.; Donald, M.; Cannon, J.; Ostrowski, S. G.; Winograd, N.; Ewing, A. G. *Anal. Chem.* **2002**, *74*, 4020–4026.
(14) Cannon, D. M. J.; Pacholski, M. L.; Winograd, N.; Ewing, A. G. *J. Am. Chem. Soc.* **2000**, *122*, 603–610.
(15) Kotter, F.; Benninghoven, A. *Appl. Surf. Sci.* **1998**, *133*, 47–57.

10.1021/ac901065s CCC: $40.75
Published on Web 06/16/2009

and detected.[16,17] Traditionally, an N of 4 was considered to be useful.[16] This concept accounts for the finite amount of ions generated for detection from small sample volumes. This definition is, however, inadequate when imaging a small number of pixels.

Keenan and Kotula have shown that consideration of counting statistics improves the quality of multivariate analyses applied to TOF-SIMS data.[18] Because SIMS images are compiled by counting relatively rare events, ions of interest striking a detector, we must consider the resulting distribution of the intensities measured. Thus, an image of a uniform surface will not appear uniform because the pixel intensities follow a binomial distribution. This distribution precludes the direct comparison of two individual pixels and complicates the interpretation of imaging data. Thus, when analyzing small volumes, one must also consider factors which influence the intensity for a molecule of interest, i.e., the surface concentration, the change in concentration expected, the effective ionization efficiency, and the spot size of the primary ion source.

In this work, we demonstrate that SIMS imaging data can be accurately modeled using the Poisson distribution. By analysis of the data in this manner, a better understanding and more robust interpretation of the surface composition is obtained. Our approach allows the identification and validation of pixel-to-pixel heterogeneity not possible with line scans. This capability allows the interrogation of lipid domains, which can appear anywhere on the cell surface and with sizes smaller than a single pixel.

To test our approach, we imaged the phospholipid and cholesterol distributions on the surfaces of RBL-2H3 mast cells. Cholesterol-rich microdomains within the plasma membrane of these cells have been hypothesized to play functionally important roles in immunoreceptor signaling in the allergic response.[19,20] However, directly observing the spatial arrangement of these domains, and the lipids that comprise them, *in situ* with good resolution and relevant chemical information has remained elusive due to their size and lifetime.[21,22] In this work, we describe our model using simulated data that allows us to predict signal and spatial resolution limitation. The presence of these multiple populations provides compelling evidence for a heterogeneous distribution of lipid species in the resting RBL-2H3 cell membrane.

MATERIALS AND METHODS

Cell Preparation for Imaging. RBL-2H3 mast cells were suspended in BSA-containing buffered saline solution (20 mM HEPES, pH 7.4, 135 mM NaCl, 5 mM KCl, 1.8 mM $CaCl_2$, 1 mM $MgCl_2$, 5.6 mM glucose, 1 mg/mL BSA) and sensitized with a 10-fold molar excess of mouse-anti-2,4-dinitrophenyl IgE. Cells were incubated for 2 h at 4 °C. Cells were then diluted (1×10^6 cells/mL), applied to 5 mm × 5 mm Si substrates, and allowed to adhere (10 min, 37.4 °C).[22] Shards containing RBL-2H3 cells were rinsed for 5 s in 18 MΩ water to remove contamination from excess media. To prevent cell rupture, the shards were quickly frozen in liquid ethane and stored under liquid nitrogen (LN_2). The samples were introduced to the ultrahigh vacuum environment of the mass spectrometer at LN_2 temperatures, as described elsewhere.[14] Once under vacuum, the samples were warmed 5 °C/min to −80 °C to remove the water with negligible crystallization. This process was monitored using a video camera mounted on a bright field microscope. When the water was removed, the sample was quickly returned to liquid nitrogen temperatures. During the cooling process, some residual water in the vacuum environment was redeposited on the sample producing a uniform layer of water on top of the cells.[23]

Langmuir−Blodgett and Physical Vapor Deposition Film Preparation. The phospholipids used include *N*-stearoyl sphingomyelin (SSM), 1-palmitoyl-2-oleoyl-*sn*-glycero-3-phosphocholine (POPC), and cholesterol (CH). The LB films used for the investigation were either pure POPC or 23% CH/47% SM/30% PC. The lipids were applied to the air−water interface, compressed to 7 mN/m, and then transferred onto hydrophilic substrates. This relatively low pressure is used to ensure the appearance of immiscible liquid phases and to ensure that the size of the domains is large enough for SIMS observation.

Physical vapor deposition (PVD) films were prepared by subliming cholesterol (Sigma-Aldrich, St. Louis, MO) contained in a crucible by resistive heating of a tungsten filament followed by deposition onto a LN_2-cooled sample stage. The film thickness was monitored using a quartz crystal microbalance (QCM) and subsequently characterized using AFM.

Mass Spectrometer. Imaging data was acquired using a Kratos Prism TOF-SIMS spectrometer (Manchester, U.K.) equipped with an In^+ liquid metal primary ion source (FEI, Beaverton, OR). The pulsed primary ion source was operated at an anode voltage of 15 kV angled at 45° to the sample. The beam was focused to approximately 300 nm in diameter and delivered 1 nA of dc current in 50 ns pulses. The sample was mounted onto a LN_2-cooled analysis stage (Kore Tech. Ltd., Cambridge, U.K.) biased at +2.5 kV, 2.5 in. from a cold trap that was also cooled with LN_2. An extraction lens, biased at −4.7 kV, collected the secondary ions which then traveled along a 4.5 m flight path and were detected with a microchannel plate (MCP) detector (Galileo Co., Sturbridge, MA).

Data Collection and Image Analysis. Mass spectrometry images were acquired by raster-scanning the primary ion beam across the sample region and collecting a mass spectrum for each pixel. The data were collected using in-house imaging software (visual C++, Microsoft, Redmond, WA). Imaging data was imported into MATLAB (Mathworks, Natick, MA) for analysis. Individual masses were plotted with their intensities displayed on a false color scale to better portray image details. Image binning was achieved by mathematically combining adjacent pixels. Histograms were created by first using an ROI tool created in LabView to select the cell or film area. The data was then exported to Microsoft Excel, and histograms were plotted and fitted using the built-in function from the Analysis ToolPak. Multiple Poisson

(16) Brunelle, A.; Touboul, D.; Laprevote, O. *J. Mass Spectrom.* **2005**, *40*, 985–999.
(17) Prinz, C.; Hook, F.; Malm, J.; Sjovall, P. *Langmuir* **2007**, *23*, 8035–8041.
(18) Keenan, M. R.; Kotula, P. G. *Surf. Interface Anal.* **2004**, *36*, 203–212.
(19) Gidwani, A.; Holowka, D.; Baird, B. *Biochemistry* **2001**, *40*, 12422–12429.
(20) Holowka, D.; Gosse, J. A.; Hammond, A. T.; Han, X. M.; Sengupta, P.; Smith, N. L.; Wagenknecht-Wiesner, A.; Wu, M.; Young, R. M.; Baird, B. *Biochim. Biophys. Acta: Mol. Cell Res.* **2005**, *1746*, 252–259.
(21) Davey, A. M.; Heikal, A. A.; Sheets, E. D. *Biophys. Soc.* **2007**, 575A–575A.
(22) Davey, A. M.; Walvick, R. P.; Liu, Y. X.; Heikal, A. A.; Sheets, E. D. *Biophys. J.* **2007**, *92*, 343–355.
(23) Piehowski, P. D.; Kurczy, M. E.; Willingham, D.; Parry, S.; Heien, M. L.; Winograd, N.; Ewing, A. G. *Langmuir* **2008**, *24*, 7906–7911.

distributions were applied to the histogram, and the means and partial contributions were allowed to vary. The solver function varied these parameters to minimize variance and thus provide the best fit.

Model Calculations. The basic equation that describes the ion yield in a static SIMS experiment was used to obtain expected yields for imaging experiments.[24]

$$I_m = I_p Y_m \alpha^+ \theta_m \eta \quad (1)$$

where the secondary ion current, I_m, is the product of the primary ion flux, I_p, the sputter yield, Y_m, the ionization probability to positive ions, α^+, the molecules' fractional concentration, θ_m, and the transmission of the instrument, η. By measuring the secondary ion yields from pure films on the mass spectrometer to be used for imaging, we can calculate an effective ionization efficiency which is the product of $Y_m\alpha^+\eta$. Assuming that images are obtained by adhering to the static limit,[24] we can use 10^{13} impacts/cm^2 for the total primary ion flux. The use of the total dosage for I_m results in the calculation of the total secondary ion yield. This leaves only the estimation of the molecules fractional concentration, which appears frequently in the literature.[25] The calculated secondary ion yield, from eq 1, can then be used in the Poisson equation for λ, to generate the probability mass function (relative number of events versus expected counts). If the expected number of ions counted is λ, then the probability of there being exactly k counts is defined by the Poisson distribution.

$$f(k;\lambda) = \frac{\lambda^k e^{-\lambda}}{k!} \quad (2)$$

When surface concentrations are considered as distributions, the potential overlap of these distributions must be estimated using a z-score to determine the accuracy of the experiment. The z-score is the difference in the means of two different populations given in the number of standard deviations. This is indicative of how accurately we can assign a pixel to a given population.

$$z = \frac{\mu_1 - \mu_2}{\sigma_m} \quad (3)$$

where μ_2 is the mean intensity of the higher concentration, μ_1 is the mean intensity of the lower concentration, and σ_m is the standard deviation calculated from the mean ion intensity. Because of the shape of the Poisson distribution, the standard deviation is equal to $\sqrt{\mu}$.

To assess the goodness-of-fit for imaging data, reduced χ^2 values were calculated. Briefly, the reduced χ^2 is the variance of the imaging data divided by the variance predicted by the Poisson distribution. Thus, reduced χ^2 values near 1 are indicative of a good fit.

RESULTS AND DISCUSSION

SIMS Imaging of Homogeneous Surfaces. Because SIMS instruments collect data by counting occurrences, the counts in individual pixels follow a discrete probability distribution. The effect of this distribution is illustrated in Figure 1. A SIMS image of a single component Langmuir−Blodgett film made from palmitoyl-oleyl-phosphatidylcholine (POPC) is shown in Figure 1A. Figure 1B shows an intensity histogram plotted from the representative SIMS image that appears in part A. On the x-axis, pixels are binned by the intensity or number of counts. The y-axis is the number of pixels at each intensity, normalized to the total number of pixels (N/N_{tot}). Displayed as an XY plot, the image (Figure 1A) appears to be a random array of intensities, and it is difficult to draw any conclusions about the nature of the analyzed surface. The black line represents the distribution predicted by the Poisson distribution using an average intensity calculated from the entire image. The theoretical curve fits the image distribution well, giving a reduced χ^2 value of 1.1. Thus, the intensity variations observed in Figure 1A are an artifact of counting statistics and the surface is homogeneous, as would be expected given that the sample is a single component Langmuir−Blodgett film. These data also demonstrate that the Poisson distribution is an accurate model of our imaging data.

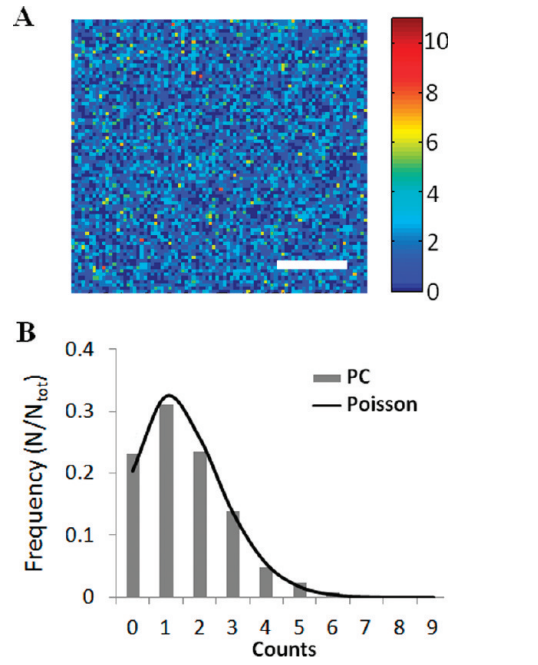

Figure 1. (A) Mass-specific image of PC from POPC LB film. (B) Histogram of signal intensity for $(m/z)^+$ 184 in a Langmuir−Blodgett film composed of POPC. The scale bar represents 100 μm.

Probability Mass Functions and Spatial Resolution. The useful lateral resolution of a SIMS imaging experiment depends upon the focus of the primary ion beam as well as the useful ionization efficiency of the molecule of interest. However, because the image is compiled by counting rare events, we must consider that the pixel intensities will follow a probability distribution. The Poisson distribution is often used to characterize the statistics of rare events with a small average number of occurrences.[26] Adopting this as our model, we can predict the results of a proposed SIMS imaging measurement to better understand the effects of the intensity distribution, surface concentration, and ionization efficiency and how these parameters will affect our measurement.

(24) Vickerman, J. C., Briggs, D., Eds. *ToF-SIMS: Surface Analysis by Mass Spectrometry*; IM Publications and Surface Spectra Limited: West Sussex, U.K., 2001.

(25) Edidin, M. *Annu. Rev. Biophys. Biomol. Struct.* **2003**, *32*, 257–283.

(26) Thompson, W. J. *Comput. Sci. Eng.* **2001**, *3*, 78–82.

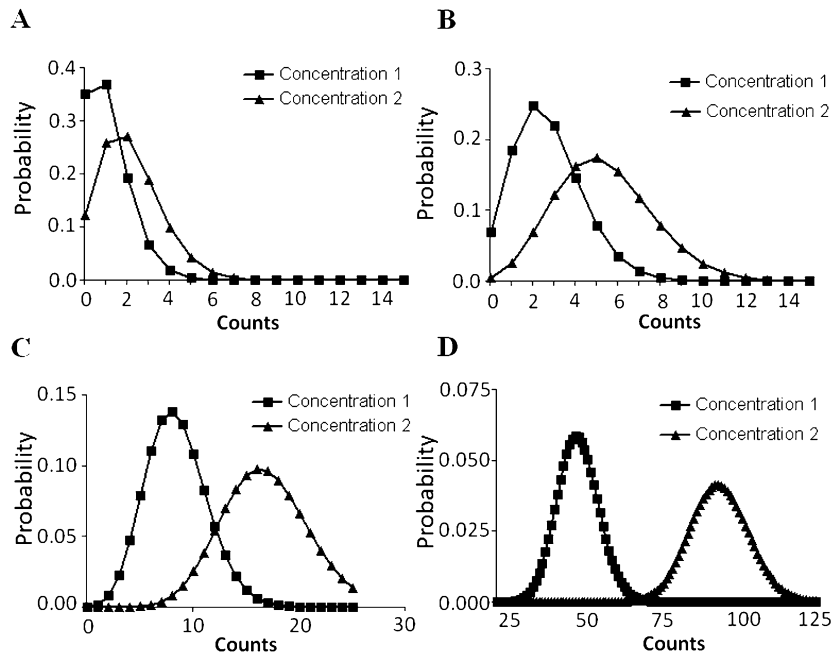

Figure 2. (A) Probability mass function for imaging cholesterol, assuming 100% concentration change between pixels, with 310 nm spatial resolution. (B) Probability mass function of two discrete populations where concentration 1 gives an average intensity of 2.67 counts and concentration 2 gives an average intensity of 5.33 counts. (C) Probability mass function for imaging cholesterol, assuming 100% concentration change between pixels, with 1.2 μm spatial resolution. (D) Probability mass function for imaging cholesterol, assuming 100% concentration change, down-binned to 2.79 μm spatial resolution.

In Figure 2, we applied our model to the theoretical imaging of cholesterol distribution in the plasma membrane of RBL-2H3 cells. The effective ionization efficiency was measured using a PVD cholesterol film imaged with an In^+ primary ion source. Although using In^+ primary ions results in lower ionization efficiencies when compared to cluster projectiles, the demonstrated compatibility with frozen sample preparations, ease of focus, and high ion currents that are routinely obtained make it useful for these experiments.

Previous work in our lab has demonstrated the m/z 147 can be used to identify cholesterol in the membrane of cryogenically preserved single cells and offers a 3-fold increase in signal intensity, when compared to the molecular ion.[27] Because of the possibility of isobaric interference when using m/z 147, it is important ensure images are free of PDMS contamination. This was achieved by scanning the total image mass spectrum for the presence of other known PDMS contamination fragments.

For this calculation, we postulated two discrete surface concentrations of cholesterol. In concentration one, cholesterol comprises 25% of the membrane lipids, while in concentration two, cholesterol comprises 50% of membrane lipids, thus corresponding to a 100% concentration change. With the use of experimentally determined ionization efficiencies and a pixel size of 310 nm, this would correspond to average pixel counts of approximately 0.6 and 1.2 for concentration one and concentration two, respectively. Figure 2A shows the expected intensity distributions calculated using these parameters. The resulting overlap of the distributions reveals that in an image containing these two populations, which differ in cholesterol concentration by a factor of 2, the two concentrations will be virtually indistinguishable. This is expected because the average pixel intensity (N) is approximately 1, and N of 4, an average of 4 counts per pixel, is required for useful lateral resolution (*vide supra*). With an increase of N to 4 for our calculations, and maintaining 100% concentration change, Figure 2B demonstrates that there is still considerable overlap. Extrapolation of this result to biological samples, which are infinitely more complex, suggests that spatial resolution estimates based on useful lateral resolution are misleading.

In Figure 2C, the spatial resolution of the data in Figure 2A has been down-binned from 310 nm to 1.2 μm by combining adjacent pixels, resulting in an N of 13.5. The plot shows that there is still an overlap in intensities. Counts in this overlap region can be differentiated with various levels of confidence; however, the majority of pixels can be identified with certainty. The degree of differentiation can be quantified using the z-score, as defined in eq 3 (Materials and Methods). For 1.2 μm spatial resolution, we calculate a z-score of 3. From numerical integration we find that a z-score of 3 corresponds to 90% separation of the two distributions. A consequence of the standard deviation having a square root dependence on the mean intensity is that, regardless of how many counts are obtained, 4 times as many are needed to double the separation between populations. The byproduct of this is illustrated in Figure 2D. To obtain complete separation of the two distributions, defined as being >99.5%, the image would have to be down-binned to 2.79 μm spatial resolution. This degree of separation gives a z-score of 5.6.

Effect of Ionization Efficiency and Concentration Change. The spatial resolution estimates reported in Figure 2 are instrument, mass, and matrix-dependent. These calculations were performed at a constant effective ionization efficiency and con-

(27) Piehowski, P. D.; Carado, A. J.; Kurczy, M. E.; Ostrowski, S. G.; Heien, M. L.; Winograd, N.; Ewing, A. G. *Anal. Chem.* **2008**, *80*, 8662–8667.

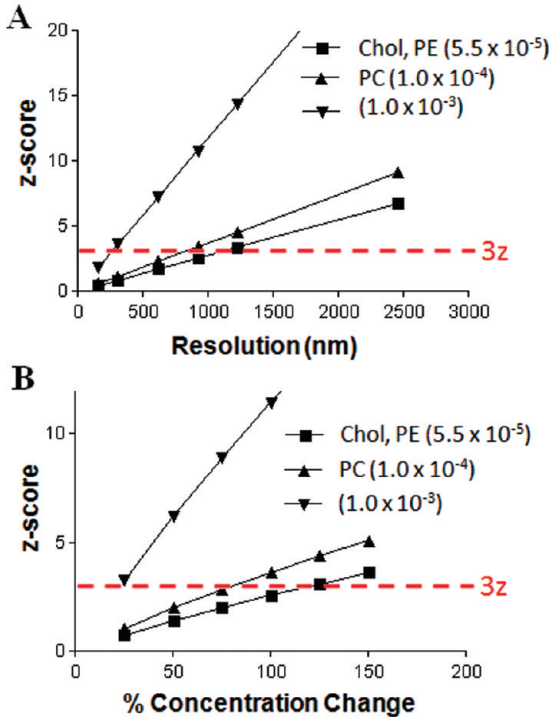

Figure 3. (A) *z*-score as a function of the lateral resolution for various lipid ionization efficiencies. The change in concentration was held constant at 100%. (B) *z*-score as a function of the change in lipid species concentration. For this plot, a spatial resolution of 1.2 μm was used, which corresponds to a *z*-score of 3, or 90% separation, for our cholesterol simulation. The numbers in the legends are ionization efficiencies.

centration change. Figure 3A shows the effect of the ionization efficiency of a species on spatial resolution. For this plot, the concentration change was again 100%, and the expected *z*-score is plotted on the *y*-axis. The demonstrated dependence on ionization efficiency results in substantially different spatial resolutions attainable for different biomolecules. Thus, in a biological experiment where measurement of the native concentration change is desired, the best way to improve lateral resolution is through increased ionization efficiencies. Ionization efficiencies for cholesterol (5.5×10^{-5}), phosphoethanolamine (5.5×10^{-5}), and phosphocholine (1.0×10^{-4}) fragments were measured using In^+ as the primary ion source. Multiple reports in the literature, i.e., utilizing cluster projectiles, MetA-SIMS, ME-SIMS, and combinations of these approaches have reported ionization efficiencies on the order of 1×10^{-3} for a number of biomolecules.[16,17,28–31] Figure 2 demonstrates that increasing ionization efficiency is promising for obtaining true submicrometer spatial resolution in biological experiments. Using a *z*-score of 3 to define our satisfactory confidence level and an ionization efficiency of 1×10^{-3}, we obtain a theoretical lateral resolution of 257 nm. In our experiment, the ionization efficiency limits the resolution to 1110 nm for cholesterol and 811 nm for phosphocholine.

(28) Altelaar, A. F. M.; Klinkert, I.; Jalink, K.; deLange, R. P. J.; Adan, R. A. H.; Heeren, R. M. A.; Piersma, S. R. *Anal. Chem.* **2006**, 734–742.
(29) McDonnell, L. A.; Heeren, R. M. A.; de Lange, R. P. J.; Fletcher, I. W. *J. Am. Soc. Mass Spectrom.* **2006**, *17*, 1195–1202.
(30) Ostrowski, S. G.; Szakal, C.; Kozole, J.; Roddy, T. P.; Xu, J. Y.; Ewing, A. G.; Winograd, N. *Anal. Chem.* **2005**, *77*, 6190–6196.
(31) Kozole, J.; Wucher, A.; Winograd, N. *Anal. Chem.* **2008**, *80*, 5293–5301.

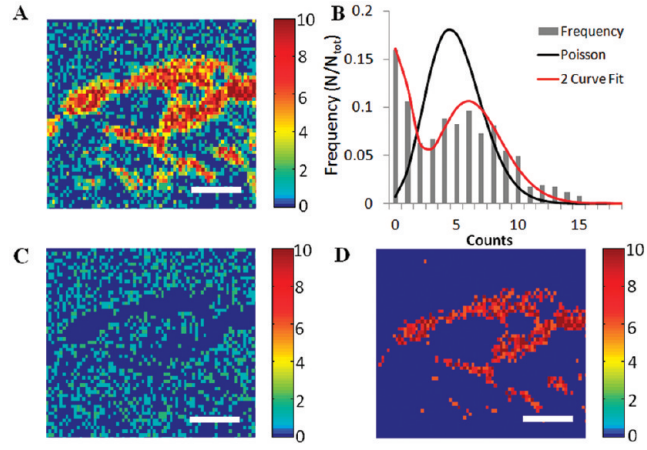

Figure 4. (A) Mass-specific image of cholesterol $(m/z)^+$ 147 in the ternary mixture of PC, sphingomyelin, and cholesterol. (B) Histogram for signal intensity of cholesterol $(m/z)^+$ 147 in a ternary mixture of PC, sphingomyelin, and cholesterol. The black line gives the predicted Poisson distribution using the average signal intensity. The red line gives the curve predicted by the Poisson distribution the two populations shown in parts C and D. (C) Map of pixels which have a cholesterol signal intensity of 0−2 counts, population 1. (D) Map of pixels which have a cholesterol signal intensity of 4−10 counts, population 2. Scale bars represent 100 μm.

We then examined the *z*-score as a function of the change in concentration of the biomolecule, while keeping a constant spatial resolution of 1.2 μm. For this calculation, concentration one was held constant at 25% and concentration two was varied from 25 to 150%. It is important to note that a smaller value for concentration one results in lower spatial resolution because it lowers the surface concentration of the molecule. This is important when considering biomolecules that are not major constituents of the sample. As one would expect, the *z*-score increases linearly with a change in concentration. This plot further emphasizes the effect of ionization efficiency; a 20% concentration change can be accurately imaged with an ionization efficiency of 1×10^{-3}, compared with 120% and 83% for 5.5×10^{-5} and 1.0×10^{-4}, respectively.

Using Histograms to Interpret Imaging Data. Although the distribution of counting data negatively impacts the spatial resolution attainable, the concept of plotting SIMS imaging data as a histogram can provide valuable information about a sample. The power of this analytical tool is demonstrated in Figure 4. Ternary Langmuir−Blodgett films have been used as model membranes for measuring lipid interactions.[32] We studied one such film made with 23% cholesterol, 47% sphingomyelin, and 30% POPC. The mass-specific image for cholesterol is shown in Figure 4A; Figure 4B contains a histogram of cholesterol intensities. Fitting the histogram with a Poisson distribution yields a reduced χ^2 value of 3.0, which suggests that multiple populations, or areas of different cholesterol concentration, are present on the surface. Indeed, the data can be fit to a model containing two distinct populations of cholesterol (Figure 4B, red trace, $R^2 = 0.96$). Mapping the pixels with intensities from 0 to 2, we obtain the image presented in Figure 4C. Figure 4D is the image from the map of pixel intensities 3−10. This demonstrates that analysis of the histogram allows us to better visualize and characterize

(32) McQuaw, C. M.; Zheng, L. L.; Ewing, A. G.; Winograd, N. *Langmuir* **2007**, *23*, 5645–5650.

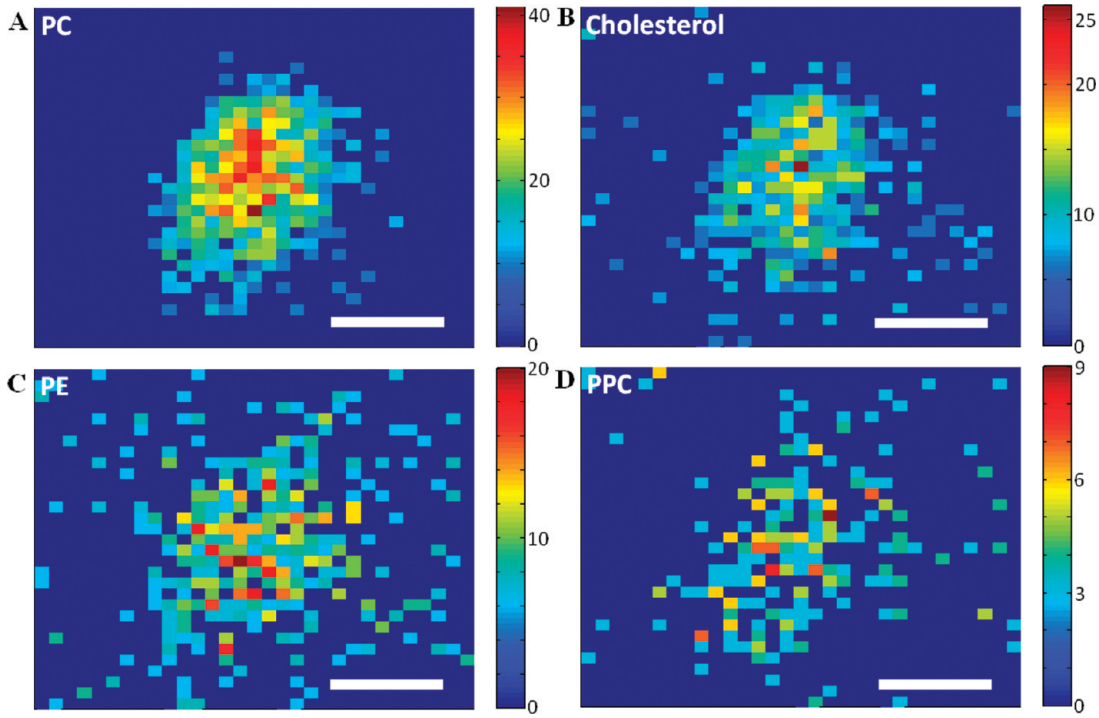

Figure 5. Mass-specific TOF-SIMS images of a RBL-2H3 mast cell. (A) PC $(m/z)^+$ 184, (B) cholesterol $(m/z)^+$ 147, (C) PE $(m/z)^+$ 142, and (C) PPC $(m/z)^+$ 224. Scale bars represent 10 μm.

domains that were previously identified via line scans,[33] giving us a complete image of the size and shape.

Single Cell Imaging of RBL-2H3 Mast Cells. One of our goals is to apply the unique capabilities of TOF-SIMS imaging to analyze the plasma membrane of single cells. These cells are 10−20 μm in diameter, and the membrane features under the experimental conditions used in the present work are submicrometer in size.[34] When imaging single cells, we are working with a small, finite sample volume. The analysis must be carried out in an ultrahigh vacuum environment, and thus great care must be exercised to preserve the arrangement of membrane components. This prerequisite precludes the use of sample pretreatments (*vide supra*) to enhance ionization efficiency. To further complicate the analysis, the size of membrane features is on the scale of micrometers and in many cases smaller. In addition, membrane components are commonly present in low concentrations on the surface. As a result, the data obtained from these experiments is often difficult to interpret. Thus, we applied our histogram analysis to identify possible populations, or domains, in the plasma membrane.

In Figure 5, four mass-specific TOF-SIMS images of a single RBL-2H3 cell are shown. The original images were collected using 310 nm pixels, as limited by the focus of the In^+ primary ion source. The images have been down-binned to 1.2 μm pixels to increase the contrast obtained. For a 100% concentration change in cholesterol, this would correspond to a separation of 3 *z*. The masses mapped represent the phosphocholine headgroup (PC), cholesterol, the phosphoethanolamine headgroup (PE), and the phosphocholine headgroup plus part of the glycerol backbone (PPC). Phosphocholine containing lipids are the most abundant species in the mammalian cell membrane,and they have the highest ionization efficiency, as evidenced in Figure 5A by the far greater intensity and contrast seen in the PC image. Examination of this image gives information about the size and morphology of the cell. Given the inherent distribution of counting data, combined with varying ionization efficiencies and surface concentrations of the lipid, it is very difficult to draw any conclusions about the lipid species distribution from the images. The commonly used method for identifying heterogeneity, line scans, is problematic on this size scale because the effects of the intensity distribution dominate the generated line profile. To decrease the counting noise in a line scan, adjacent pixels are averaged resulting in a smooth profile. This approach is effective when analyzing domains much larger than a single pixel and having a characteristic location.[2,3] However, this averaging obscures the information contained in single pixels and therefore decreases the spatial resolution. To identify smaller features, a new approach is needed.

Single Cell Histograms. To gain further insight into the lipid distribution, we generated intensity histograms for each of the species mapped and show these in Figure 6. To do this, a region of interest was selected and the intensities for each pixel were then exported to statistical software. The boundary of the cell is derived from the boundary of the PC map for reasons specified above. Secondary ion micrographs (data not shown) confirm that RBL-2H3 cells present a flat surface to the analysis beam. To further minimize cell edge effects on the histogram, the outermost pixel around the cell perimeter was omitted. With analysis of cells that are not adherent and flat, further considerations will be required to account for the effect cell morphology on secondary ion collection efficiency. The mean pixel intensity was again used

(33) Zheng, L.; McQuaw, C. M.; Ewing, A. G.; Winograd, N. *J. Am. Chem. Soc.* **2007**, *129*, 15730.
(34) Davey, A. M.; Krise, K. M.; Sheets, E. D.; Heikal, A. A. *J. Biol. Chem.* **2008**, *283*, 7117–7127.

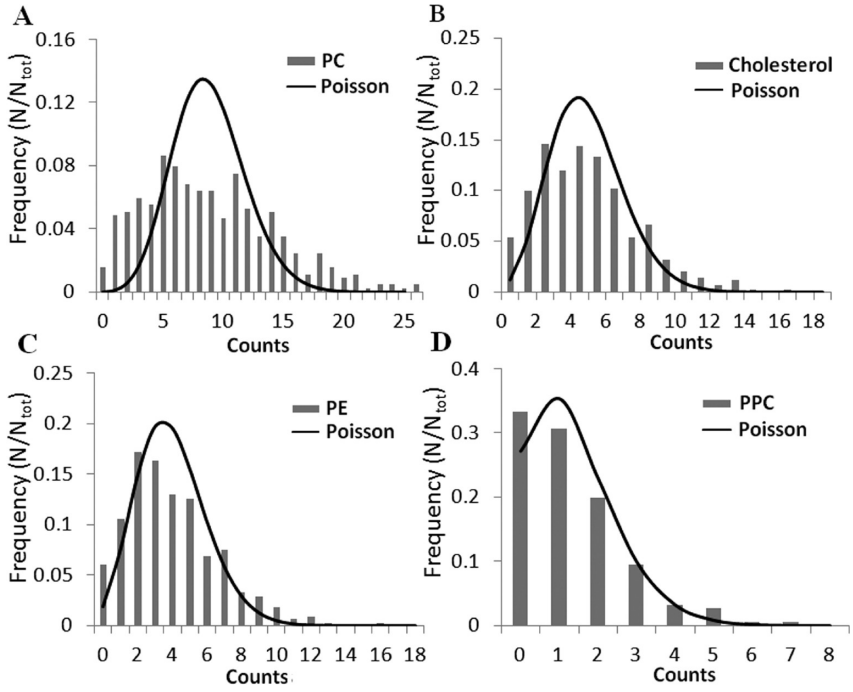

Figure 6. Histograms of the four lipid masses mapped in Figure 4. Histograms are the result of 452 pixels. The theoretical Poisson distribution, generated using the average pixel intensity, is overlaid in black. (A) $(m/z)^+$ 184, PC, (B) $(m/z)^+$ 147, CH, (C) $(m/z)^+$ 142, PE, and (D) $(m/z)^+$ 224, PPC.

Table 1. Reduced χ^2 Values for Lipids Imaged in the RBL-2H3 Cell

	mast cell 1	mast cell 2	mast cell 3	mast cell 4	mast cell 5	average ± SD
PC	3.30	2.18	2.19	2.35	2.30	2.46 ± 0.47
cholesterol	1.95	2.01	1.62	1.99	1.66	1.85 ± 0.19
PE	1.81	1.94	1.73	1.63	1.71	1.76 ± 0.12
PPC	1.39	1.71	1.35	1.30	1.49	1.45 ± 0.16

to generate the theoretical curve predicted by the Poisson distribution to demonstrate the expected intensity distribution from a homogeneous surface. Because each pixel is treated as an independent measurement, the histograms reported in Figure 6 have an n of 452.

It is apparent from the PC histogram that there is significant heterogeneity in the distribution of PC-containing lipid species across the surface of the cell. Reduced χ^2 analysis gives a value of 3.30, indicative of the poor fit. Because of the complexity of the PC histogram, interpreting the biological significance of this result is not possible at this time. Histograms of cholesterol and PE similarly suggest heterogeneous surface distributions of these species, with reduced χ^2 values of 1.95 and 1.81, respectively. The distribution of cholesterol intensities is discussed in further detail below. The fit for the PPC histogram, with a reduced χ^2 value of 1.39, suggests a more homogeneous distribution. Because of the low average intensity of PPC, a z-score of <1 is expected for a 100% concentration change. Thus, large variations in concentrations could be concealed in this histogram, and the result must be qualified in this manner. Table 1 displays the reduced χ^2 values for RBL-2H3 cell images shown in Figure 5, along with four other representative sets of RBL-2H3 cell images. The corresponding histograms for the cholesterol maps are presented in Figure 6.

Matrix Effects in Single Cell Plasma Membrane Imaging. When imaging with TOF-SIMS, it is necessary to consider the influence of matrix effects. It is imperative that the ionization efficiency of the analyte is constant across the surface of the cell to conclude that varying analyte concentration causes fluctuations in ion intensity. The cellular membrane is a tightly regulated, highly organized bilayer structure. The result is that lipids in a membrane consistently arrange themselves in the same orientation, perpendicular to the surface with hydrophilic moieties directed away from the interior. This leads to a repeating packing structure, which provides a consistent number of nearest neighbors with similar chemical properties.[35] If the presence of membrane proteins on the cell surface, when averaged over the pixel area, is assumed to be approximately constant. Given these two assumptions, lipids in the plasma membrane are found in similar chemical environments. Thus, if the membrane is well preserved with cryogenic sample preparation methods, it can be argued that matrix effects in all pixels across the surface are equivalent.

To demonstrate this, the pixels that were in the top 10% of signal intensity for each of the four lipids mapped in Figure 5 were plotted in different colors, Figure 7A–D. The identity of each lipid mass is listed in the figure legend. This image demonstrates that these pixels are well distributed across the surface of the cell, regardless of the lipid moiety, thus validating our assumption that the ionization environment for lipids is relatively uniform across the cell. If the various lipid species ionization efficiencies were not constant across the cell surface, we would expect that high-intensity pixels would appear as clusters on the surface. To further illustrate this lack of clustering, the four lipid masses are

(35) Gennis, R. B. *Biomembranes: Molecular Structure and Function*; Springer: New York, 1989.

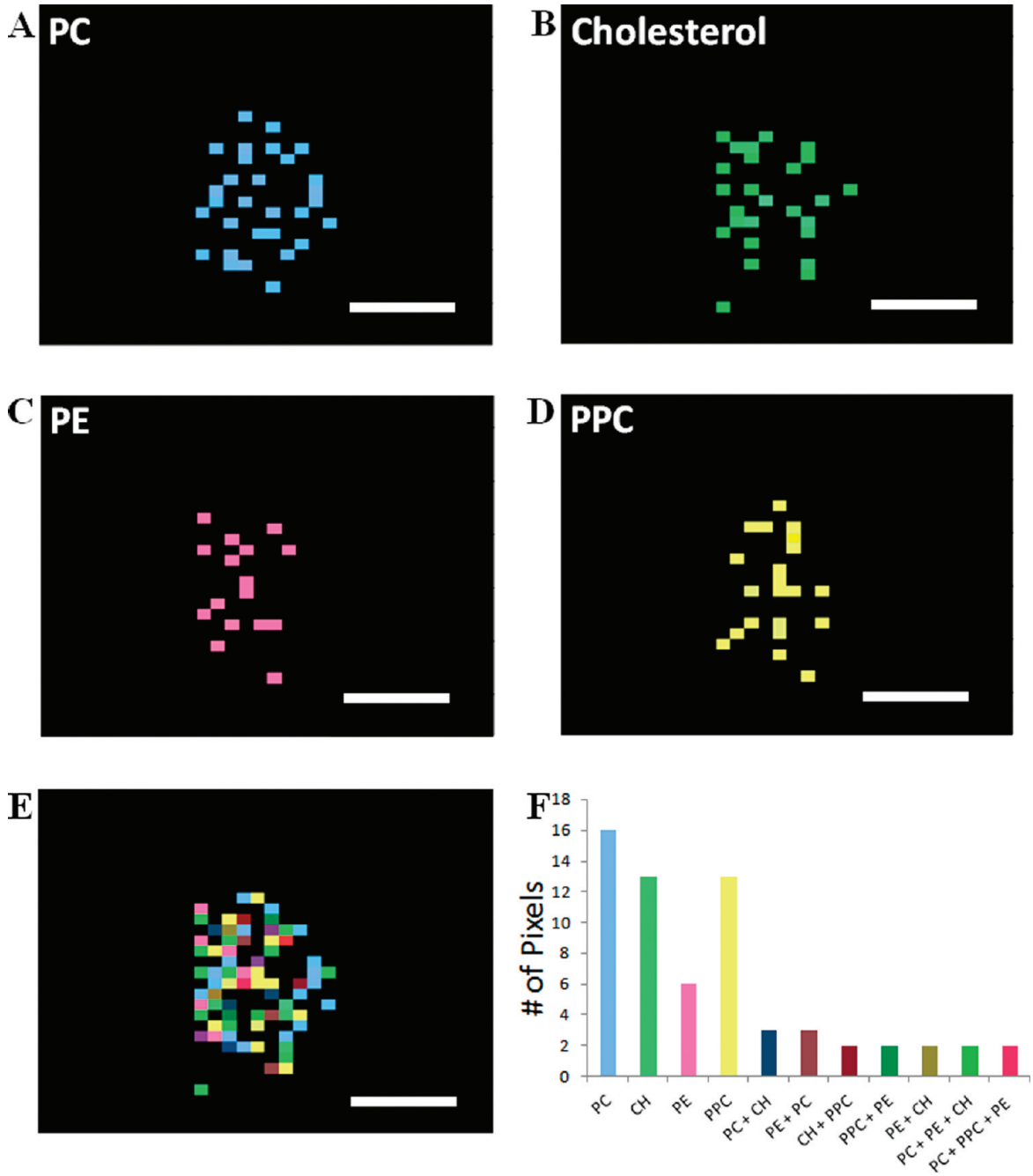

Figure 7. Pixels in the top 10% of signal intensity for (A) PC $(m/z)^+$ 184, (B) cholesterol (CH) $(m/z)^+$ 147, (C) PE $(m/z)^+$ 142, and (D) phospholipid only derived PC $(m/z)^+$ 224. (E) Overlay of parts A–D. (F) Histogram of the coincidence of high-intensity lipid signals. The extended color legend can be seen below the histogram. Scale bars represent 10 μm.

overlaid in Figure 7E. Pixels where overlap occurs are represented by new colors. The occurrence of overlap is then summarized with a histogram in Figure 7F. The identity of the colors is listed below the corresponding bar in the histogram. Figure 7F demonstrates that high intensity pixels most often occur exclusively, which also argues against the existence of ionization hotspots.

Distribution of Cholesterol in RBL-2H3 Mast Cells. The histograms produced from cholesterol images suggest the presence of multiple populations or domains in the membrane. To extract more information from the histograms they were fit using multiple Poisson distributions. The mean and fractional surface contribution of the populations were allowed to vary to minimize error and produce the best fit. Figure 8A gives the resulting correlation coefficient as a function of molecular populations used. This plot demonstrates that the data are well described using three populations, and improvement in correlation coefficient is negligible when more curves are employed. This result is consistent for all five cholesterol images analyzed. Thus, the three-parameter model was adopted. An example of the three-curve fit is shown in Figure 8B. The three component curves are shown in Figure 8C to give an idea of the relative contribution of each population. The results obtained for all the images, $n = 5$, are summarized in Figure 8D. Examining the means from the fit curves reveals that population 1 has approximately half the cholesterol concentra-

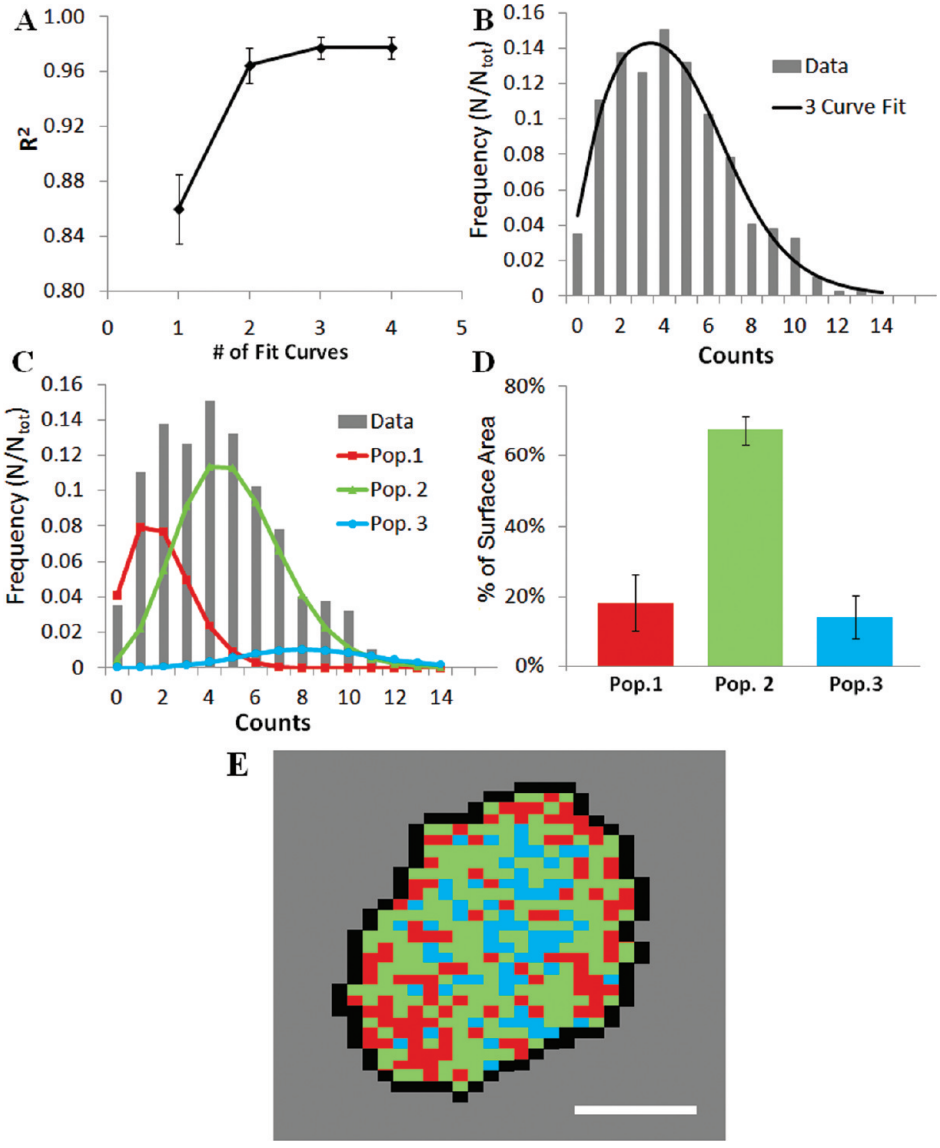

Figure 8. (A) A plot of correlation coefficient vs number of weighted distributions used to fit cholesterol intensity distribution histograms. (B) Representative cholesterol histogram with a three parameter fit shown in solid black, $R^2 = 0.98$. (C) The three curves that compose the three parameter fit shown in Figure 6B. (D) Bar plot demonstrating the expected surface coverage for each cholesterol intensity population. (E) Reconstructed cell image displaying the locations of the three populations on the surface. The black outline corresponds to the boundary of the cell defined by the PC signal, which was used to generate the histogram. The color scheme for the populations is conserved from part D. For this image, population 1 is defined as pixels containing intensities 0−3, population 2 is 4−7, and population 3 is 8−13. The scale bar is 10 μm. For parts A and D, $n = 5$ and the error bars denote standard deviations.

tion of population 2, and population 3 has twice the cholesterol concentration of population 2 (data not shown).

FRET and ESR studies indicate that as much as 65% of the cell surface may exist as cholesterol-rich domains in resting mast cells.[36] In addition, it is likely that nanoscopic segregation of these phases occurs in live cells.[37] Therefore it is important to describe the surface distribution of cholesterol in resting RBL-2H3 mast cells. The results shown in Figures 5, 6, and 8 as well as Table 1 demonstrate that heterogeneity in the lipid distribution of resting mast cells is observed by SIMS imaging. In the case of cholesterol, the evidence suggests that L_o domains exist on the cell surface, and even in the absence of cross-linking, heterogeneity in their surface distribution exists. A very important caveat for our TOF-SIMS imaging results is that the RBL-2H3 cells were treated for 2 h at 4 °C, which likely leads to quasi-phase separation that is cold-induced.[38,39] Indeed, plotting the pixels that correspond to each of the population intensities allows a map of these domains to be generated (Figure 8E). It is interesting to note that the higher intensities (population 3) are central in the cell, the lowest (population one seem to locate mostly around the outer parts of the cell, and the intermediate intensities (population two) are more spread out across the cell. This representation certainly

(36) Swamy, M. J.; Ciani, L.; Ge, M. T.; Smith, A. K.; Holowka, D.; Baird, B.; Freed, J. H. *Biophys. J.* **2006**, *90*, 4452–4465.
(37) Sengupta, P.; Holowka, D.; Baird, B. *Biophys. J.* **2007**, *92*, 3564–3574.
(38) Bali, R.; Savino, L.; Ramirez, D. A.; Tsvetkova, N. M.; Bagatolli, L.; Tablin, F.; Crowe, J. H.; Leiday, C. *Biochim. Biophys. Acta, Biomembr.* **2009**, *1788*, 1229−1237.
(39) Gousset, K.; Tsvetkova, N. M.; Crowe, J. H.; Tablin, F. *Biochim. Biophys. Acta* **2004**, *1660*, 7–15.

appears to show heterogeneity based on the amount of cholesterol in specific domains of the membrane, a significant finding.

CONCLUSIONS

When interpreting SIMS images, it is essential to consider the intensity distribution of the molecular fragments. The distribution becomes increasingly important as the sample area becomes smaller and affects the attainable spatial resolution. The primary ion source spot size, the ionization efficiency of the analyte, the surface concentration, and the change in surface concentration to be measured are all important. Modeling can provide information about the feasibility of the experiment as well as the confidence level of the result. This approach uses a simple Poisson distribution to model the pixel intensity distributions obtained from SIMS imaging of homogeneous surfaces. A more detailed representation of the surface is obtained by plotting the image intensity distributions as a histogram. Populations identified from histograms can be mapped to reveal unique distributions that are difficult to ascertain from the mass-specific images.

Plotting mass-specific images obtained from RBL-2H3 reveals that the lipid distribution on the plasma membrane is inhomogeneous. The evidence is especially strong in the case of PC-containing lipids. Although the nature and origin of these heterogeneities is presently unclear, SIMS imaging suggests the presence of substantial surface concentration differences in the plasma membrane. Histograms of cholesterol share the common characteristic of a small population of pixels exhibiting a 2-fold increase in signal intensity. This provides direct evidence for the presence of cholesterol-rich domains on the cell surface.

ACKNOWLEDGMENT

This work was supported by grants from the National Institutes of Health (Grant 2R01EB002016-16, N.W. and A.G.E, and Grant AG030949, E.D.S.) and the National Science Foundation (Grant MCB 0718741, E.D.S). The authors thank Carolyn McQuaw and Leilang Zheng for the use of their Langmuir−Blodgett film images. The authors also thank John Vickerman for valuable discussions of the manuscript. A.G.E. is supported as a Marie Curie Chair from the European Union 6th Framework.

SUPPORTING INFORMATION AVAILABLE

Total ion images for a homogeneous POPC film, ternary film, and RBL-2H3 cell. This material is available free of charge via the Internet at http://pubs.acs.org.

Received for review May 15, 2009. Accepted June 10, 2009.

AC901065S